Materials Transactions, Vol. 43, No. 10 (2002) pp. 2536 to 2542

Formation and Annealing Behavior of Nanocrystalline Steels Produced by Ball Drop Test

Minoru Umemoto *, Xinjiang Hao, Tomohiro Yasuda and Koichi Tsuchiya

Department of Production Systems Engineering, Toyohashi University of Technology, Tempaku-cho, Toyohashi 441-8580, Japan

Nanocrystallization by a ball drop test in an eutectoid steel with either pearlite or spheroidite structure has been studied. By a ball drop test, nanocrystalline layer has been formed along the surface (near the edge of the impact crater) and interior of specimen (near the bottom of the impact crater). Prior deformation of specimens has been found to reduce the number of ball drops to produce nanocrystalline layer. When the prior deformation was severe enough, one time of ball drop could produce a nanocrystalline layer. Severe shear deformation was observed at the nanocrystalline layer. This suggests that strain localization under a high strain rate deformation promotes nanocrystallization. For the samples with pearlite structure, cementite dissolved completely in the nanocrystalline layer. For the samples with spheroidite structure, most of cementite particles also dissolved by a ball drop test. A mechanism account for dissolution of spherical cementite is proposed. After annealing at 873 K for 3.6 ks, grain growth took place in the nanocrystalline region in contrast to recrystallization in work-hardened region like observed in ball milled powders. Fine cementite particles re-precipitated at nanocrystalline ferrite grain and then inhibited the grain growth effectively.

(Received April 15, 2002; Accepted August 6, 2002)

Keywords: *cold working, microstructure, steel, nanocrystalline, ball drop, annealing, cementite dissolution*

1. Introduction

Grain refinement could greatly improve materials properties, especially when refined to nanometer regime. Severe plastic deformation is an effective way to refine grains to submicrometer or even nanometer. Among the various severe plastic deformation methods, extensive works have been carried out on the formation of nanocrystalline structures by ball milling due to its simplicity, low cost, and applicability to essentially all classes of materials.[1,2] However, the contamination during ball milling and the grain growth during sintering the milled powders limit the engineering application of ball milled powder. Recently, a number of new processing methods, such as equal channel angular pressing (ECAP),[3] severe plastic torsion straining (SPTS)[4] and accumulative roll bonding (ARB)[5,6] have been developed to produce bulk ultra fine grained materials. These methods offer several significant advantages, including reduced susceptibility to contamination and the elimination of sintering process. However, the grains fabricated by these methods are usually in the range of one hundred to several hundreds nanometers and not actual nano-sized. To develop severe plastic deformation methods to produce real bulk nanocrystalline materials, detailed understanding of the mechanism and conditions of nanocrystallization induced by ball milling is desired. We[7–11] have studied the microstructural evolution and nanocrystallization of Fe–C alloys by ball milling. Layered nano-structure has been found as transitional microstructure from work-hardened to equiaxed nanocrystalline structure. A critical dislocation density is considered to exist to induce nanocrystallization by deformation.[7–11] High strain rate may be one of the necessary conditions to achieve this critical dislocation density.[4,10,11] However, the deformation mode in ball milling process is substantially complicated and it is hard to analyze the amount of strain, strains rate, temperature rise and its duration *etc*. To overcome these difficulties, a ball drop test was carried out to simulate the ball milling process, in which a ball with a weight was dropped onto a bulk specimen repeatedly.[12]

In our previous paper,[12] we reported that nanocrystalline structure similar to that obtained by ball milling was found in eutectoid steel specimens after a number of ball drops. A high strain rate of around $10^4\,s^{-1}$ was proposed to be an essential condition to produce nanocrystalline structure by deformation. Further studies have been carried out on the nanocrystallization by a ball drop test. In the present paper, we report, 1) the location of nanocrystalline region with respect to ball impact crater, 2) the effect of pre-strain on the number of ball drops to produce nanocrystalline region, and 3) annealing behavior of the nanocrystalline region formed by a ball drop test.

2. Experimental Procedures

The material used in this study was an eutectoid carbon steel (Fe–0.80C–0.25Si–0.50Mn in mass%) with either pearlite or spheroidite structure. The pearlite structure was obtained by patenting treatment. Specimens were austenitized at 1223 K for 1.8 ks followed by an isothermal transformation to pearlite at 873 K for 0.3 ks in a lead bath. The spheroidite structure was produced by a process of martensite tempering, in which specimens were austenitized at 1173 K for 3.6 ks and quenched into water to obtain martensite, and then tempered at 983 K for 79.2 ks. To study the effect of prestrain on the formation of nanocrystalline structure by a ball drop test, specimens were rolled to various reductions by multipass rolling (with 10% or 20% reduction per pass) before a ball drop test. Specimens after a ball drop test were sealed in quartz tubes with pure Ar protective atmosphere and annealed at 873 K for 3.6 ks.

In a ball drop test, the weight with a ball attached on its bottom was dropped from a height of 1 or 2 m onto bulk spec-

*Corresponding author: E-mail: umemoto@martens.tutpse.tut.ac.jp

imens with flat surface. The ball of 6 mm in diameter, the weight of either 4 or 5 kg and the specimens with 15 mm in diameter and 2 to 4 mm in thickness were used. When a ball was dropped more than two times on a specimen, a specimen was shifted horizontally or vertically by 2 mm step for each drop test.

All tests were carried out at room temperature in air. The details of the ball drop test were described in our previous paper.[12] Specimens were characterized by scanning electron microscope (SEM, JEOL JSM-6300), atomic force microscope (ATM, Shimazu SPM-9500) and Vickers microhardness tester (MVK-G1 with an applied load of 0.98 N for 10 s). Specimens for SEM and AFM observations were etched by 5% Nital.

3. Experimental Results

3.1 Location of nanocrystalline region after ball drop test

The nanocrystalline region formed by a ball drop test usually appears near the surface of specimens. A typical nanocrystalline region formed by a ball drop test is shown in Fig. 1. These SEM micrographs (cross section) were taken from the specimen with pearlite structure after 8 times of ball drops with a weight of 4 kg from a height of 1 m. A layer (dark appearance under SEM) with a thickness of about 10 μm is seen along the surface near the edge of the impact crater (Fig. 1(a)). This type of layer was confirmed as nanocrystalline region by TEM observation as reported previously.[12] Near the bottom of the crater (Fig. 1(b)), the nanocrystalline layer locates several tens of micrometers beneath the surface. Although the typical location of nanocrystalline region is like shown in Fig. 1, the location is different from specimen to specimen. The reason of this is that several times of ball drops are required to initiate nanocrystallization. The surface of specimen initially flat becomes rough when the nanocrystalline region starts to form and this resulted in the irregular shape and various locations of nanocrystalline region. Thus it is desired to produce nanocrystalline region by one time of ball drop to make the deformation condition simple.

To try to produce nanocrystalline regions by one time ball drop, specimens were pre-strained by cold rolling. Figure 2 shows some of such results, where the specimens were pre-strained by rolling (20% reduction per pass) with reduction of 77% (Fig. 2(a)) and 82% (Fig. 2(b)) before one time of ball drop (5 kg weight from a height of 1 m). The hardness of specimens after rolling was 3.9 GPa and 4.2 GPa for 77% and 82% rolling reduction, respectively. The nanocrystalline layer on the surface of a specimen is clearly seen in Fig. 2(b) but not detectable in Fig. 2(a). From the experiment using specimens with various rolling reduction, it was concluded that rolling reduction of about 80% is a critical degree of prior deformation to produce nanocrystalline layer by one time of ball drop with 5 kg weight and 1m height. The hardness of the nanocrystalline layer produced by one time of ball drop is usually lower (6.1 GPa) than that of after ball dropped several times (> 9 GPa). It seems that higher degree of deformation is needed to produce fully nanocrystalline region.

Figure 3 shows the nanocrystalline layers formed symmetrically along the ball falling axis in a specimen rolled to 82%

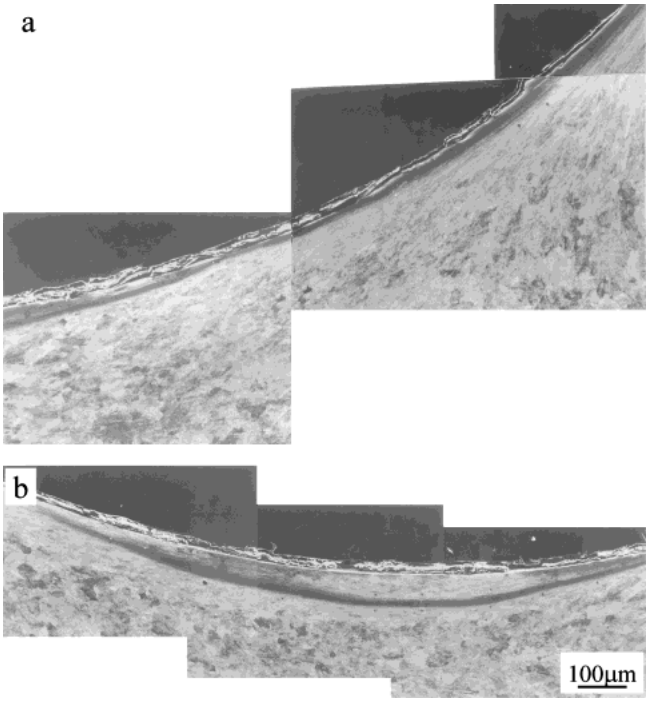

Fig. 1 Nanocrystalline layer in the sample with pearlite structure after 8 times of ball drops (4 kg, 1 m) (a) at the edge of crater and (b) at the bottom of crater.

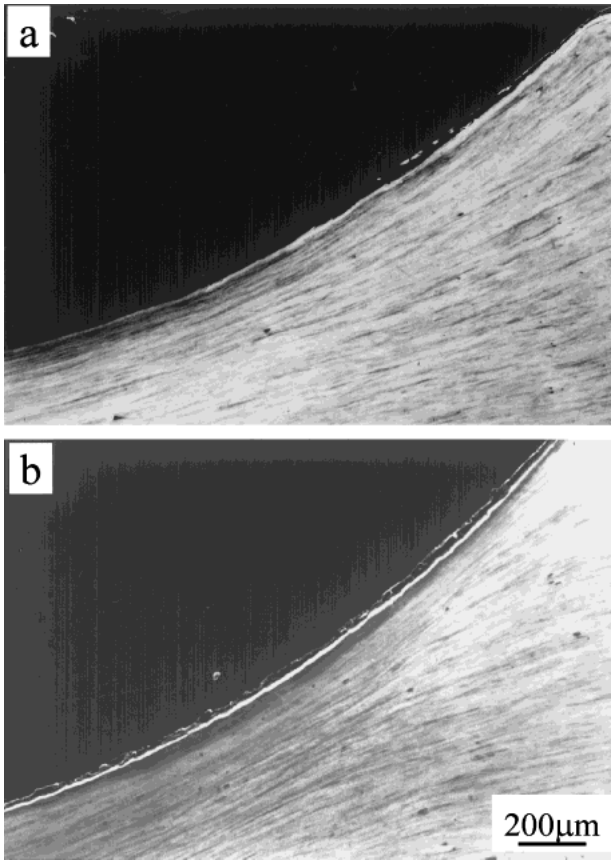

Fig. 2 Nanocrystalline layer in the samples with pearlite structure after cold rolling to (a) 77% and (b) 82% reduction and one time of ball drop (5 kg, 1 m).

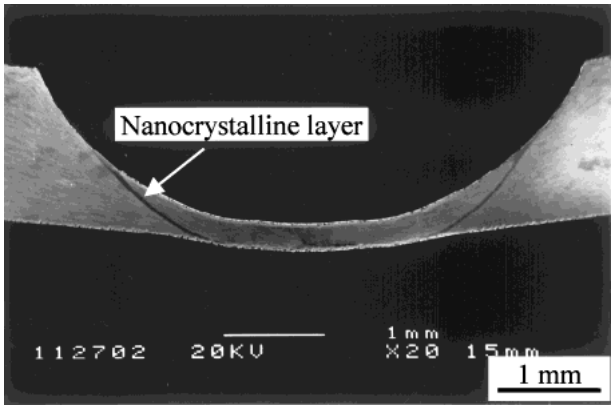

Fig. 3 Nanocrystalline layer in the sample with pearlite structure after cold rolling to 82% reduction and one time of ball drop (5 kg, 2 m).

(25% reduction per pass and final thickness 1.8 mm) and one time of ball drop (5 kg, 2 m). The nanocrystalline layer appeared along the surface of the crater edge and then penetrated to the bottom surface of the specimen. If the sample has an enough thickness, the whole nanocrystalline layer may form inside the sample like shown in Fig. 1. Regretfully, thicker samples with the same rolling reduction could not be produced because of the limit in roll gap of the mill used in the present study.

3.2 Shear deformation in nanocrystalline layer

Large shear is observed around the nanocrystalline layer produced by a ball drop test as is shown in Fig. 4. Figure 4(a) shows a nanocrystalline layer observed in a sample (without pre-strain) with pearlite structure after 3 times of ball drops (5 kg, 1 m). The hardness of the dark contrast nanocrystalline layer is about 10 GPa and that of matrix is about 5 GPa. The matrix is work hardened since the hardness of the sample before the ball drop test was about 3 GPa. It should be noted that the pearlite lamellar structure is clearly seen in the work harden regions but the lamellar structure is unrecognizable in the nanocrystalline layer.

The amount of shear in the nanocrystalline layer can be estimated when it forms in the pre-strained specimens with pearlite structure. When cold rolled pearlite structure is etched, a fine stripe pattern like shown in Fig. 4(b) appears. The difference in etched contrast arises probably from the difference in interlamellar spacing of lamellae and each stripe corresponds to each pearlite colony. Using this strip pattern the amount of shear strain in nanocrystalline layer can be estimated. Figure 4(b) shows the nanocrystalline layer observe in a sample with pearlite structure after prior cold rolling (80% reduction, 10% per pass) and one time of ball drop (5 kg, 1 m). Using the measured angle θ of 7°, the amount of shear strain, γ, of the layer was calculated from the relation $\gamma = 1/\tan(\theta)$ to be 8.1. Since the hardness of the layer shown in Fig. 4(b) (7.4 GPa) is not high enough, the shear strain should be greater than 8 to produce thorough nanocrystalline layer like shown in Fig. 4(a). Taking the pre-strain of 80% rolling reduction (1.9 in true strain) into account, the true strain necessary to produce nanocrystalline layer is estimeted to be larger than 3.1.

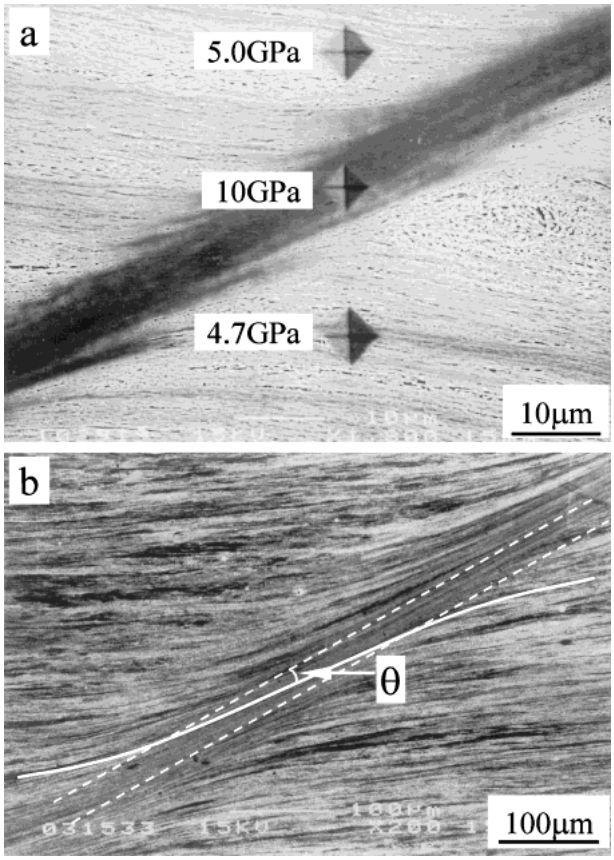

Fig. 4 Shear deformation in the samples with pearlite structure after ball drop (5 kg, 1 m) (a) 3 times without prior deformation and (b) 1 time with prior deformation (80% rolling reduction, 10% per pass).

3.3 Annealing behavior of ball dropped samples

The samples after a ball drop test were annealed at 873 K for 3.6 ks. Figure 5(a) shows a typical SEM micrograph of a sample with pearlite structure. It was found that after annealing, the microstructures of work-hardened region and nanocrystalline region are still quite different and there is a clear boundary between the two regions. In the work-hardened region, recrystallization and grain growth of ferrite took place, leading to recrystallized ferrite grains with an average size of about 0.5 μm. Simultaneously, the spherodization of lamellar cementite took place. The average size of cementite particle is about 0.2 μm. In contrast, a much fine microstructure is seen in the prior nanocrystalline region, where fine cementite particles are re-precipitated. The microstructure in Fig. 5(a) is quite similar to that observed in the ball milled samples after annealing as shown in Fig. 5(b) (Fe–0.89C pearlite steel powders ball milled 360 ks and annealed at 873 K for 3.6 ks).[7] The cementite volume fraction in the prior nanocrystalline region shown in Fig. 5 (and Fig. 6) looks larger than that in the prior work-hardened region although those are the same. One reason is that the cementite particle size in the prior nanocrystalline region is much finer (less than 50 nm) than that in the prior work-hardened region (0.1–0.2 μm). The bright contrast of cementite observed by SEM makes the cementite particles look larger than the real. As a consequece, the apparent volume fraction is larger in the prior nanocrystalline region than that in the prior work-hardened region. The second reason is that

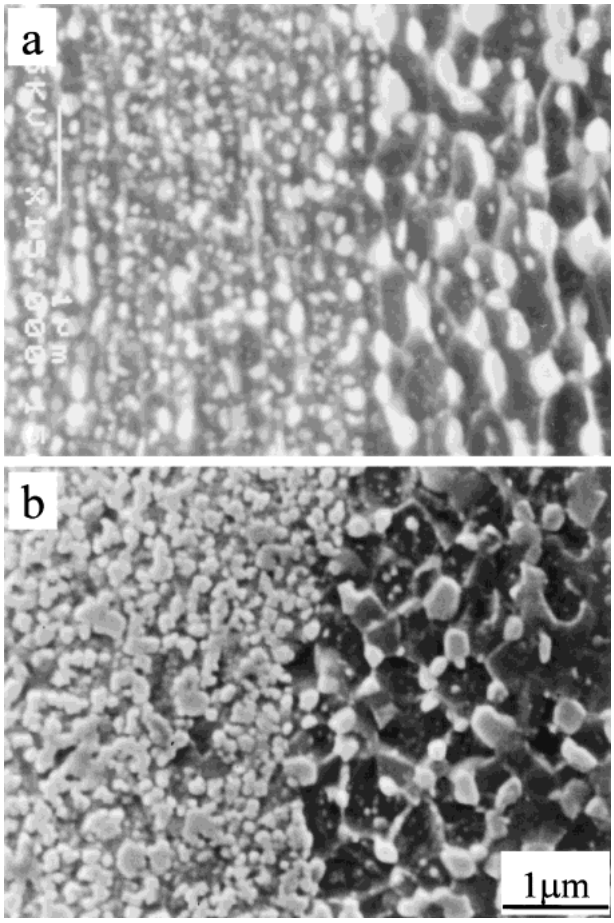

Fig. 5 Annealed (873 K for 3.6 ks) microstructures of the samples with pearlite structure after deformation (a) 30 times of ball drops (5 kg, 1 m) and (b) Fe–0.89C ball milled for 360 ks.

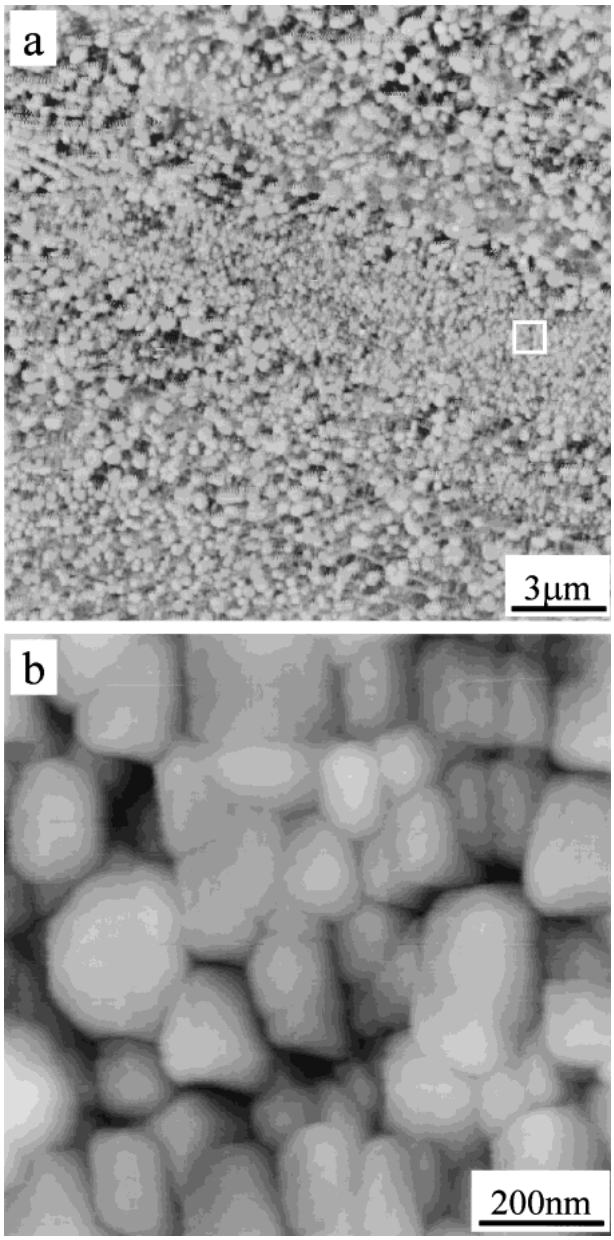

Fig. 6 AFM images of the sample with pearlite structure after 30 times of ball drops (5 kg, 1 m) and annealing at 873 K for 3.6 ks.

in the nanocrystalline region the areas without grain growth looks similar with the re-precipitated cementite. During annealing, the SEM contrast of nanocrystalline region changes from dark to bright due to grain growth. The areas where a certain grain growth takes place become dark contrast. The nanocrystalline areas without grain growth appears as islands (about 0.1 μm in diameter) with bright contrast. Those areas look similar with the re-precipitated cementite as is typically shown in Fig. 5(b). These two reasons make the volume fraction of cementite in the prior nanocrystalline region look larger.

Figure 6(a) is an AFM image of Fe–0.80C pearlite sample annealed at 873 K for 3.6 ks after 30 times of ball drops (5 kg, 1 m). Similar to SEM micrographs, cementite particles and ferrite grains were observed in work-hardened region. Figure 6(b) is an enlarged image of the nanocrystalline region marked in Fig. 6(a). Grains with an average diameter of 130 nm were clearly seen. Since the size of cementite particle is similar to ferrite grain, it is difficult to distinguish them.

Similar microstructural change by annealing was observed in the specimens with spheroidite structure. Figure 7(a) shows a microstructure of a specimen ball dropped 50 times (5 kg, 1 m) and annealed at 873 K for 3.6 ks. It was noted that two kinds of cementite particles, very fine cementite particles ($< 0.2\,\mu m$) and bigger cementite particles ($> 0.5\,\mu m$), appear in the nanocrystalline region (left hand side). The ferrite grains around bigger cementite particles have an average size of about 0.5 μm. It was considered that the bigger cementite particles were those not dissolved by the ball drop test and the cementite particles with less than 0.2 μm in diameter are those re-precipitated from ferrite. The microstructure of Fe–0.89 wt%C steel with spheroidite structure after ball milling and annealing is shown in Fig. 7(b).[11] In the nanocrystalline region (left hand side), the microstructure of the ball-milled specimen is finer than that of ball dropped specimen. It was noticed that an annealed microstructure formed from spheroidite structure is coarser than that from pearlite structure.

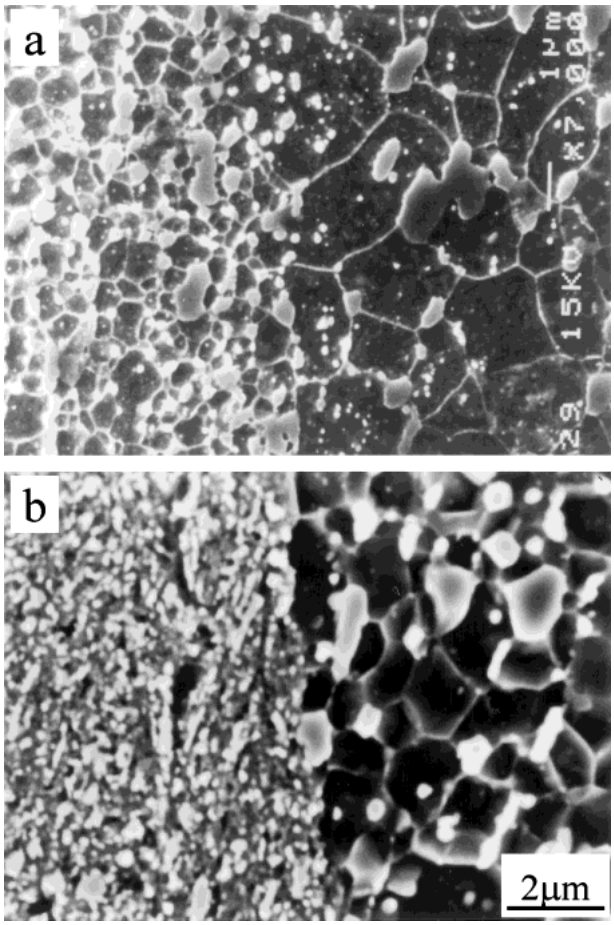

Fig. 7 Annealed (873 K for 3.6 ks) microstructures of the samples with spheroidite structure after deformation (a) 50 times of ball drops (5 kg, 1 m) and (b) Fe–0.89C ball milled for 360 ks.

4. Discussion

4.1 Mechanism of nanocrystallization induced by deformation

Severe plastic deformation is one of the promising methods to produce bulk nanocrystalline materials. In spite of a large number of works done on fabricating nanocrystalline materials by deformation, the mechanism is not well understood yet. Only a few researchers considered the mechanism account for nanocrystallization by severe plastic deformation. Fecht *et al.*[13] described the nanocrystallization by ball milling dividing the process into the following three stages. 1) Initially, the deformation is localized in shear bands consisting of an array of dislocations with high density. 2) At a certain strain level, these dislocations annihilate and recombine to small angle grain boundaries separating the individual grains. During this process the strain built up in the small crystallites decreases due to the lowering of the dislocation density. The subgrains formed via this route are already in the nanometer size range. During further milling the areas having small grains extend throughout the entire sample volume. 3) At last, the orientations of the grains with respect to their neighboring grains become completely at random. Valiev *et al.*[14] proposed a model on the nanocrystallization by severe plastic deformation (ECAP, SPTS) with the emphasis on the transformation of cellular structure to granular structure. During deformation, when the dislocation density in the cell walls reaches a certain critical value, a partial annihilation of dislocations of different signs occurs at the cell boundaries. As a result, excess dislocations of single sign remain. The excess dislocations play various roles: dislocations with Burgers vector perpendicular to the boundary lead to an increase of misorientation and when their density rises they cause the transformation to a granular structure; at the same time, long range stress fields are connected with glide dislocations which can also lead to sliding of grains along grain boundaries.

In the above two models, it was shown that two steps play the key roles in nanocrystallization. First, a critical dislocation density should be attained for cellular structure transforms to granular structure. Second, grains should rotate randomly with large angle to achieve random orientation. In our previous study on ball milling steel powders,[11] it was found that during ball milling a layered nanocrystalline structure first formed and then equiaxed nanocrystalline structure is gradually produced by the subdivision of layered nanostructure. The problems are how to increase dislocation density to a critical value and how to enhance grain rotation to make random orientation.

It was considered that a high strain rate is advantageous to increase dislocation density and grain rotation. Several works about the effects of strain rate on the dislocation density and grain rotation have confirmed this. Chiem[15] studied the flow stress of single crystals deforming in shear at a number of constant strain rates in the range of 10^{-5}–$1600\,s^{-1}$ and to strains of about 20%. They found a linear increase in flow stress (equivalently dislocation density) with the logarithm of strain rate up to $500\,s^{-1}$, followed by a more rapid increase at higher strain rates. Lee *et al.*[16] also found the flow stress of AISI 4340 high-strength alloy steel increases more rapidly when the strain rate greater than $10^3\,s^{-1}$. Canova *et al.*[17] performed a computer simulation on the effect of strain rate on slip system activity and lattice rotation and found that higher strain rates promote lattice rotation in simple shear to a greater extent than lower strain rates. This is due to the increase in the number of activated slip systems, which leads to greater lattice rotations.

From the above consideration, it is clear that a high strain rate is preferable to obtain a high dislocation density and a large grain rotation. In the present study it was found that a pre-strain has a significant effect on the nanocrystallization by a ball drop test. The number of ball drops necessary to produce nanocrystalline region decreased with increasing the degree of pre-strain. To produce nanocrystalline layer by one time of ball drop, the degree of pre-strain should exceed a critical value as shown in Fig. 2. This indicates that to reach a critical dislocation density, a large degree of deformation is necessary together with a high strain rate. The dislocations introduced by pre-strain rolling clearly contribute to reach a critical dislocation density necessary for nanocrystallization, although the prior-strain may also contribute to increase the strain rate of a ball drop test by harden the samples and shorten the impact time.

4.2 Mechanism of cementite dissolution during a ball drop test

In the present study, it was demonstrated that the cementite could dissolve partially or completely even by one time of ball drop. The duration of deformation is very short, in the order of 10^{-4} s, as estimated in previous study.[12] A question is how the cementite can dissolve in such a short time, especially large cementite particles in spheroidite structure.

Cementite dissolution is a common phenomenon in pearlitic steels during heavy plastic deformation processes, such as wire drawing,[18] ball milling,[19] high-pressure torsion[20] and surface friction[21] *etc*. Intensive works have been done on the cold drawn pearlitic steel wire since it posses a high strength of more than 5 GPa together with acceptable toughness. It has been found that cementite dissolution is strongly related with the abnormally high work hardening ability and stain aging strengthening of the pearlite steel wire. Several mechanisms on the cementite dissolution have been proposed. Gridnev *et al.*[22] first proposed that the interaction between C atoms and dislocations is responsible for cementite dissolution. According to them, the interaction energy between a carbon atom and dislocation in ferrite matrix is larger than the binding energy between carbon and iron atoms in cementite. Then, carbon atoms may migrate from cementite to ferrite with dislocations moving out from the cementite lamellae into ferrite during deformation or diffuse out from cementite to dislocations located in ferrite near the ferrite-cementite interface. During low temperature annealing, cementite will further dissolve and carbon will pin dislocations and cause stain age hardening. Recently, Languillaume *et al.*[23] proposed another interpretation based on the destabilization of cementite phase during deformation. By applying intensive plastic deformation to pearlite, the thinning of the cementite lamellar as well as the formation of slip steps on the interface of the cementite lamellae occurs. The free energy of the cementite phase is increased by an interfacial contribution to such an extent that cementite becomes unstable and dissolves into ferrite. Hidaka *et al.*[24] also proposed that cementite can dissolve by deformation due to the increase in the specific interfacial energy. They further proposed that C atom might be segregated to nanocrystalline ferrite grain boundaries to form amorphous layer, which will decrease the grain boundary energy since the interface energy between crystalline and amorphous phase is one order of magnitude lower than the conventional grain boundary energy.

The thickness of lamellar cementite in pearlite structure is usually several tens of nanometer and is thin enough to be deformed plastically. Its size is further reduced by severe plastic deformation and might become smaller than the critical nucleus size of cementite when nucleates from carbon supersaturated ferrite. Besides the size reduction, the interfacial energy of α/θ itself might increases by deformation due to the loss of coherency. Destabilization of cementite might further be enhanced by lattice defects, such as dislocations, vacancies and internal stresses induced by deformation. The carbon concentration in cementite might be reduced by deformation and will destabilize cementite substantially. From above reasons, it seems possible that the lamellar cementite in pearlite dissolves in a short time during ball drop impact. However, for the specimens with spheroidite structure, most of cementite particles are quite big (with an average diameter of 1 μm). It is not reasonable to consider that the same mechanisms can explain the dissolution of large cementite particles. Based on microstructural observations, a mechanism responsible for spherical cementite dissolution by ball drop test is suggested as follow. By the impact force of ball drop, cementite particles first fracture into small pieces. When the cementite particles become small enough, slip deformation becomes possible and cementite starts to deformation plastically. The specific interfacial energy of cementite increases by particle size refinement. When the free energy increase of cementite reaches to such an extent (> 10 kJ/mol), cementite becomes unstable and starts to dissolve.

There are several possible locations for carbon atoms in a specimen after cementite dissolution, such as around dislocations, at grain boundaries, conventional interstitial site in ferrite, *etc*. DSC analyses[9] showed that the peak temperature corresponds to cementite precipitation in ball milled nanocrystalline powders (around 650 K) is higher than that in martensite (around 580 K). It infers that the state of C atoms in nanocrystalline structure is different from that in martensite. Gridnev *et al.* suggested if carbon atoms segregate to dislocations, the re-precipitation temperature is at around 670 K, which is close to that observed in our experiment using the nanocrystalline powders. However, in the ball milled nanocrystalline Fe–C alloy powders, dislocations were scarcely observed by TEM and HREM observations. It seems not possible that most of C atoms segregate to dislocations. It was considered that in nanocrystalline Fe–C alloy most of C atoms segregate to grain boundaries and the grain boundaries become amorphous phase when cementite dissolved completely.

5. Conclusions

Nanocrystallization by a ball drop test was studied using eutectoid steel with either pearlite or spheroidite structure. It was found that nanocrystalline layer forms along the surface (near the edge of the impact crater) and interior of specimen (near the bottom of the impact crater). Prior deformation of the specimen reduces the number of ball drops to produce nanocrystalline layer. When the prior deformation is severe enough, one time ball drop could produce nanocrystalline layer. Severe shear deformation is observed at the nanocrystalline layer. This suggests that strain localization by high strain rate deformation assisted the nanocrystallization. For the samples with pearlite structure, cementite dissolved completely in nanocrystalline layer. For the samples with spheroidite structure, most of cementite particles also dissolved in the nanocrystalline region. A mechanism account for dissolution of spherical cementite has been proposed. After annealing at 873 K for 3.6 ks, grain growth takes place in the nanocrystalline region in contrast to recrystallization in work-hardened region.

Acknowledgments

This study is financially supported in part by the Grant-in-Aid by the Japan Society for the Promotion of Science.

REFERENCES

1) C. C. Kock: Nanostructured Mater. **9** (1997) 13–22.
2) C. Suryanarayana and C. C. Kock: *Non-equilibrium processing of materials*, (Pergamon, Oxford, 1999) pp. 313–346.
3) O. V. Mishin, V. Yu. Gertsman, R. Z. Valiev and G. Gottstein: Scr. Mater. **35** (1996) 873–878.
4) R. Z. Valiev, R. K. Islamgaliev and I. V. Alexandrov: Prog. Mater. Sci. **45** (2000) 103–189.
5) Y. Saito, H. Utsunomiya, N. Tsuji and T. Sakai: Acta Mater. **47** (1999) 579–583.
6) N. Tsuji, Y. Saito, H. Utsunomiya and S. Tanigawa: Scr. Mater. **40** (1999) 795–800.
7) M. Umemoto, Z. G. Liu, K. Masuyama, X. J. Hao and K. Tsuchiya: Scr. Mater. **44** (2001) 1741–1745.
8) Z. G. Liu, X. J. Hao, K. Masuyama, K. Tsuchiya, M. Umemoto and S. M. Hao: Scr. Mater. **44** (2001) 1775–1779.
9) M. Umemoto, Z. G. Liu, X. J. Hao, K. Masuyama and K. Tsuchiya: Mater. Sci. Forum **360–362** (2001) 167–174.
10) J. Yin, M. Umemoto, Z. G. Liu and K. Tsuchiya: ISIJ Int. **41** (2001) 1389–1396.
11) Y. Xu, Z. G. Liu, M. Umemoto and K. Tsuchiya: Metall. Mater. Trans. **33A** (2002) 2195–2203.
12) M. Umemoto, B. Huang, K. Tsuchiya and N. Suzuki: Scr. Mater. **46** (2002) 383–388.
13) H. J. Fecht, E. Hellstern, Z. Fu and W. L. Johnson: Adv. Powder Metall. **2** (1989) 111–122.
14) R. Z. Valiev, Yu. V. Ivanisenko, E. F. Rauch and B. Baudelet: Acta Mater. **44** (1996) 4705–4712.
15) C. Y. Chiem and J. Duffy: Mater. Sci. Eng. **57** (1983) 233–247.
16) W. S. Lee and H. F. Lam: J. Mater. Proc. Tech. **57** (1996) 233–240.
17) G. R. Canova, C. Fressengeas, A. Molinari and U. F. Kocks: Acta Metall. **36** (1988) 1961–1970.
18) V. N. Gridnev and V. G. Gavrilyuk: Phys. Metals **4** (1982) 531–551.
19) H. Hidaka, T. Suzuki, Y. Kimura and S. Takaki: Mater. Sci. Forum **304–306** (1999) 115–120.
20) A. V. Korznikov, Yu. V. Ivanisenko, D. V. Laptionok, L. M. Safarov, V. P. Pilyugin and R. Z. Valiev: Nanostructured Mater. **4** (1994) 159–167.
21) W. Lojkowski, M. Djahanbakhsh, G. Burkle, S. Gierlotka, W. Zielinski and H. J. Fecht: Mater. Sci. Eng. **A303** (2001) 197–208.
22) V. N. Gridnev, V. V. Nemoshkalenko, Yu. Ya. Meshkov, V. G. Gavrilyuk, V. G. Prokopenko and O. N. Razumov: Phys. Status Solidi A **31** (1975) 201–210.
23) J. Languillaume, G. Kapelski and B. Baudelet: Acta Mater. **45** (1997) 1201–1212.
24) H. Hidaka, Y. Kimura and S. Takaki: J. Iron Steel Inst. Japan **85** (1999) 52–58.